Journal of Materials Science: Materials in Medicine (2018) 29:82
https://doi.org/10.1007/s10856-018-6091-z

BIOMATERIALS SYNTHESIS AND CHARACTERISATION

Original Research

Sol–gel based calcium phosphates coatings deposited on binary Ti–Mo alloys modified by laser beam irradiation for biomaterial/clinical applications

Marcio Luiz dos Santos[1,2] · Carla dos Santos Riccardi[3] · Edson de Almeida Filho[4] · Antonio C. Guastaldi[4]

Received: 20 July 2017 / Accepted: 24 May 2018 / Published online: 11 June 2018

Abstract

Ti-15Mo alloy samples were irradiated by pulsed Yb: YAG laser beam under air and atmospheric pressure. Calcium phosphate coatings were deposited on the irradiated surfaces by the sol–gel method. The sol was prepared from the precursors Ca $(NO_3)_2.4H_2$ O and H_3 PO_4. The modified surfaces were submitted to heat treatment conditions at 350 and 600 °C. The results showed that the two conditions established have a sufficient energy to promote ablation on the laser beam irradiated surfaces. Likewise, it has been demonstrated the processes of fusion and fast solidification from the laser beam irradiation, under ambient atmosphere, inducing the formation of stoichiometric TiO_2 and non-stoichiometric titanium oxides, including Ti_3O_5, TiO, Ti_3O and Ti_6O with different oxide percentages depending on the fluency used. Besides that, laser modification has allowed a clean and reproducible process, providing no traces of contamination, an important feature for clinical applications. The physico-chemical and morphological properties indicated the formation of a mixture of phases: calcium pyrophosphate, hydroxyapatite and β-TCP for the procedure (PA: calcination temperature), whereas HA (hydroxyapatite) and β-TCP (tricalcium phosphate) were obtained by the procedure (PB: calcination temperature). Therefore, it was possible to obtain a Ti-15Mo alloy surface consisted on calcium phosphate ceramics of biological interest using the procedure (PB). Thus, the laser beam irradiation associated to bioactive coatings of calcium phosphates of biological interest have shown to be promising and economically feasible for use in dental and orthopedic implants.

Graphical Abstract

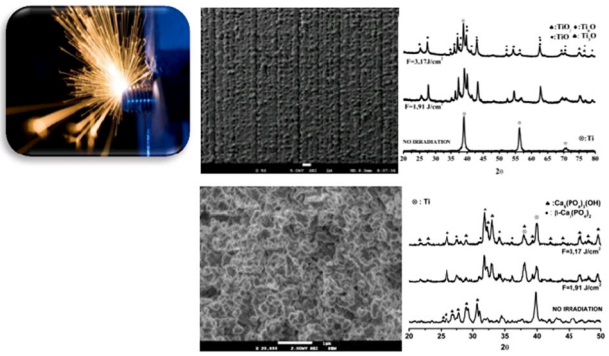

✉ Marcio Luiz dos Santos
marcsant08@gmail.com

[1] Center of Natural and Human Sciences, Federal University of ABC – UFABC, 09210-580 Santo André, São Paulo, Brazil

[2] Biotechnology and Innovation in Health Program and Master Professional in Pharmacy Program - Anhanguera University of São Paulo (UNIAN – SP), 05145-200 São Paulo, SP, Brazil

[3] College of Agricultural Sciences, Paulista State University – UNESP, 18610-307 Botucatu, São Paulo, Brazil

[4] Institute of Chemistry, 14800-060, Biomaterials Group, Paulista State University – UNESP, Araraquara, Brazil

1 Introduction

The demand for artificial implants in humans is increasing, due to the increase of the world population, and the loss of functions of the body due to the process of aging and accidents [1, 2]. The materials used as biomaterials should have certain desirable properties, such as biocompatibility, biofunctional, bioadhesion, adequate and compatible mechanical properties with bone, processability and resistance to corrosion, and especially added-market value [3, 4]. The Ti-15Mo alloy is one of the most promising for implant applications due to electrochemical stability behavior in simulated body fluid media. It is directly associated to biocompatibility as an essential condition for the use of an implantable biomaterial. However, the biological response from the surface interactions of the biomaterial/biological environment should be further evaluated despite the development of Ti–Mo alloys has allowed obtaining materials with mechanical properties, resistance to corrosion, modulus of elasticity and biocompatibility suitable for application as biomaterial. In this context, it is important to use surface modification methods to improve the biological activity of these materials, promoting osseointegration [5–10].

Additionally, the contamination of titanium surfaces and their alloys using traditional texturization techniques has influenced researchers to develop techniques that do not require different chemical elements. Considering this requirement, laser beam irradiation can provides a great tool due to concentrated beam of light, which only requires a physical medium to propagate. Preliminary studies indicated similar results to those found in others traditional applied texturization techniques [10, 11]. However, it was possible to obtain a significantly lower degree of surface contamination by laser irradiation. The most common types of lasers comprehend those generated by a gas mixture containing carbon dioxide, as well as those generated by Nd: YAG (Neodymium —Yttrium Aluminum Garnet) and Yb: YAG solid. The CO_2, Yb: YAG and Nd: YAG lasers can be used in cutting, welding and surface modification applications [12].

The surface modification of (unalloyed commercially pure Ti) cp Ti (and its alloys can be obtained by laser beam irradiation. However, it is necessary to establish the correct relation between the parameters of the beam (frequency, time of application, energy and intensity) and the obtained composition and morphology of the irradiated surface. In the cell adhesion process to biomaterials, the surface properties, such as topography and surface energy play a fundamental role in the osteoblastic adhesion that occurs in osseointegration [3, 13, 14].

The literature has reported a correlation of the parameters of the laser beam, the atmospheric conditions and the formation of oxide phases, as well as the surface morphology [9, 15–17].

The sol-gel method allows to deposit materials while at the same time also enabling one to control their structural, textural and morphological properties [18, 19]. Several articles have been published using the sol-gel method with different precursors to obtain calcium phosphate coatings [19–25]. On basis in the present work, the surface of the Ti-15Mo alloy was modified by laser beam Yb:YAG, in order to characterize new morphologies and the formation of calcium phosphate. The deposition of bioactive ceramics of calcium phosphates was accomplished using dip-coating sol-gel method. The influence of the heat treatment on the formation of the calcium phosphate on Ti-15Mo surfaces was evaluated.

2 Materials and methods

2.1 Laser-activated surface modification

Samples of titanium alloy ($8 \times 8 \times 2$ mm) were submitted to Yb:YAG multipulse laser irradiation using a Laser *Omni-Mark* 20 F ($\lambda = 1090$ nm). The topography is related to surface morphology and roughness, and surface energy, depending on the phases formed [26, 27]. All surfaces were modified under pressure and air atmospheric conditions. The parameters (power, frequency and scan speed) with two fluency (ablation) values of 1.91 and 3.17 J/cm^2, Table 1. The laser parameters were set according to the procedure proposed by Braga [28]. After irradiation, the samples were treated ultrasonically and separately in solutions of ethyl alcohol, acetone and distilled water, followed by oven-drying, and characterization.

2.2 Coating of samples by the sol gel method

The sol used was prepared from the reaction $Ca(NO_3)_2.4H_2O$ and H_3PO_4, dissolved in methanol (reaction 1). The preparation of the sol-gel solution was performed with a stoichiometric calcium/ phosphorus ratio of 1.67. The pH of the calcium phosphate precursor sol was, approximately, 2.0.

$$10\,Ca(NO_3)_2.4H_2O_{(s)} + 6H_3PO_{4_{(l)}} \xrightarrow[CH_3OH]{} Ca_{10}(PO_4)_6(OH)_{2_{(aq)}} + 20HNO_{3_{(aq)}} + 38H_2O_{(l)} \quad (1)$$

The samples, without and after laser beam irradiation, were cleaned by ultrasonic process using sequential solutions of

Table 1 Fluency obtained by irradiation of the laser beam

Samples	0	1	2
Fluency (J/cm^2)	–	1.91	3.17

Table 2 Preparation of calcium phosphate coatings

Process	Immersions	Calcination (°C) /ST
PA	4	350 °C/60 min.
PB	4	600 °C/60 min.

ST stay time (min)

neutral detergent-distilled water, Milli-Q water and acetone-ethanol (1: 1), and dried in air. For the deposition of the calcium phosphate coatings, the dip-coating technique was used. The substrates were immersed in the sol-gel solution at a constant rate of 52 mm/min and 60 s of immersion.

In the study, two procedures were used, Table 2:

- Procedure A (PA): after each immersion, the samples were calcined at 350 °C, removal of the muffle furnace, the sample was expected to cool, and four times repeatedly processed.
- Procedure B (PB): after each immersion, the sample was calcined at temperature of 600 °C, removed of the muffle furnace, the sample was expected to cool and four times repeatedly processed.

2.3 Characterization

All coated and uncoated samples were characterized by scanning electron microscopy (SEM), using a Zeiss EVO LS-15, Oxford Inca Energy 250. The X-ray diffraction analysis was performed in a Siemens D5000 X-ray diffractometer, using a scan angle of 20 at 80° with a step size of 0.02 (2θ). Each sample was subjected to a counting time of 10 s/step in a Bragg-Brentano configuration, using Cu (kα1) radiation. Quantification by Rietveld refinement was performed in a Rigaku RINT-2000 X-ray diffractometer with rotating anode, operating under the experimental conditions at 42KV, 120 mA, with divergence slits, scattering angle of 0.5°, 5 mm horizontal opening of the divergence slit, 0.3 mm receiving signal, 5° Soller, copper anode, and wavelengths of $K\alpha_1 = 1.55056$ Å and $k\alpha_2 = 1.5444$ Å, $I\alpha_2/I\alpha_1 = 0.5$. The chemical bonds of the calcium phosphates coatings were characterized by vibrational infrared spectroscopy, using a Bruker Vertex 70 FTIR spectrophotometer equipped with a diffuse reflection DRIFT Collector™.

3 Results

3.1 Laser surface irradiation

Figure 1 shows the micrographs (SEM) of the sample without laser irradiation (0 sample) and with irradiation (1.91 and 3.17 J cm^{-2}). It was observed an increase of energy density (higher fluency), provides an increase in irregularity surface with different levels of roughness (ablation).

Figure 2 shows the diffractograms of control samples (without irradiation) and samples 1 and 2 (1.91 and 3.17 J/cm^2), respectively. It can be verified in the laser beam-treated surfaces the ablation process has modified the topography, and produced the formation of stoichiometric and non-stoichiometric oxides as predicted by the fluency equation [28]. X-ray diffraction spectra revealed, in addition to β-Ti peaks (#: 89-4913), the presence of β -TiO (#: 89-5010), Ti_3O (#: 76-1644), Ti_6O (#: 72-1471), TiO_2 (#: 77-441) [29].

Table 3 shows the oxide phases percentage obtained by Rietveld refinement, corresponding to laser beam-irradiated surfaces [30].

3.2 Coating using the sol gel method

The preparation of the sol using the precursors $Ca(NO_3)_2.4H_2O$ and H_3PO_4, and methanol as solvent, produces a homogeneous solution of pH ≈ 2. According to Kanazawa [31], in solution containing phosphate and calcium ions with pH lower than 6.6, there is a predominant formation of the monohydrogen calcium phosphate dihydrate phase (DCPD—$CaHPO_4.2H_2O$). Thereby, it is possible the transformation in other phases under thermal treatment, such as calcium pyrophosphate, tricalcium phosphate (TCP), octacalcium phosphate, hydroxyapatite (HA) and hydroxyapatite deficient in calcium (HA_D).

3.2.1 Procedure (PA)—heat treatment at 350 °C

Figure 3 shows the diffractograms of the bioactive coatings, submitted to the procedure (PA). In all samples the peaks corresponding to the phases of the Ti-15Mo alloy (#: 89-4913), a mixture of calcium pyrophosphate phases (#: 17-499; 45-1061), HA (#: 89-4405) and β-TCP (#: 70-2065) were identified [29]. It can be observed the samples irradiated with laser beam promote the formation of phases of calcium phosphates. Calcium pyrophosphate, Ca/P ratio = 1.0, belongs to the group of condensed phosphates, compounds having P-O-P bond. These are formed by the condensation of monohydrogen calcium phosphate with increasing temperature, reactions 2 and 3 [20, 32].

The spectra in the mid-wave infrared region of the bioactive coatings submitted to the procedure (PA) are shown in Fig. 4. It can be observed bands in the regions from 595 to 1115 cm^{-1}, corresponding to the vibrational mode PO_4^{3-} [23, 33]. Thus, the formation of inorganic salts, according to XRD analysis, can confirm the presence of tricalcium phosphate phase. Bands in the regions

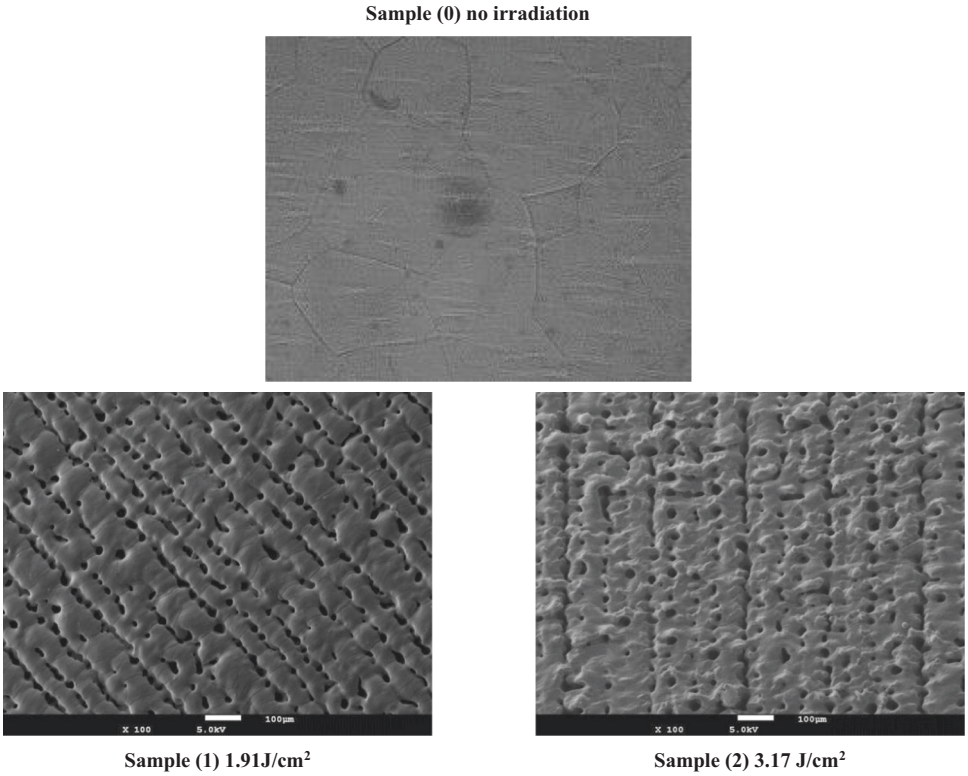

Fig. 1 SEM of the Ti-15Mo alloy without irradiation (0) and (1) 1.91and (2) 3.17 J / cm^2. Magnitude 100×

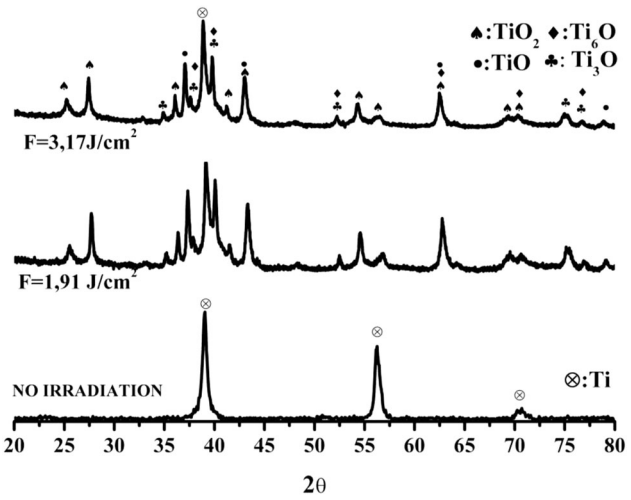

Fig. 2 **X**-ray diffraction sample (0) no irradiation, samples (1) 1.91 and (2) 3.17 J/cm^2

between 1100-960 and 725 cm^{-1} indicate the asymmetric stretching of the P-O-P bond, as well as a band assignment in the region of 1240 cm^{-1}, the P=O group. So, it was confirm the presence of the pyrophosphate group in coatings, according to DRX results (Fig. 3). In all samples (0, 1 and 2), the presence of the band was verified at 3572 cm^{-1}, which is associated to the stretching vibration of the OH group of the hydroxyapatite phase. In the fingerprint region, the presence of 632 and 595 cm^{-1} was observed. These bands are related to the stretching of the OH group, the

Table 3 Percentage of phases composed of Ti and O after refinement by Rietveld

Fluency (J.cm^{-2})	1.91	3.17
Phases	Sample 1 (%)	Sample 2 (%)
Ti_3O	47.58	42.61
Ti_6O	23.19	23.46
TiO_2	18.89	22.39
β -TiO	10.34	11.54

vibration of the PO_4^{3-} group and the unfolding of the PO_4^{3-} group, respectively. Therefore, it could be refer to the formation of the hydroxyapatite phase [25, 34]. The bands at 1385 and 1460 cm^{-1} may be associated with CO_3^{2-} vibration from CO_2 in the atmosphere during the processes of dissolution, agitation, reaction and calcination [33–36].

Figure 5 shows the micrographies of samples 0, 1 and 2 after bioactive coatings, submitted to the procedure (PA). A mixture of spherical aggregates and dense plates were observed. This features may be related to the phases calcium pyrophosphate, HA and β-TCP [24, 31, 37].

3.2.2 Procedure (PB)—heat treatment at 600 °C

In order to obtain majority formation of the HA and β-TCP phases, the coatings were obtained by procedure (PB).

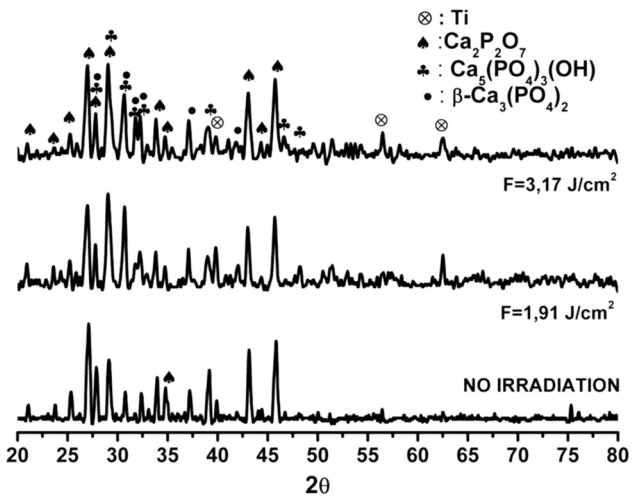

Fig. 3 X-ray diffraction of the coated samples by the sol-gel method, procedure (PA) heat treatment at 350 °C. (0) no irradiation, samples (1) 1.91 and (2) 3.17 J/cm^2

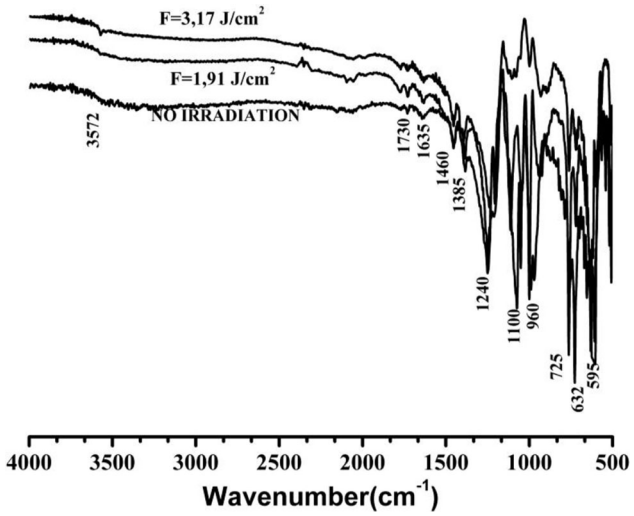

Fig. 4 Absorption spectrum in the mid-wave infrared (Mid-FTIR) region of the coated samples by the sol-gel method, procedure (PA), heat treatment at 350 °C. (0) no irradiation, samples (1) 1.91 and (2) 3.17 J/cm^2

Figure 6 shows the X-ray diffraction patterns of the bioactive coatings submitted to the procedure (PB). It is possible to observe the presence of peaks, corresponding to the Ti-15Mo alloy (#: 89-4913), a mixture of phases consisting of HA (#: 89-4405) and tricalcium phosphate (β-TCP) (#70-2065) [29].

The spectra in the Mid-infrared region of the bioactive coatings submitted to the procedure (PB) are shown in Fig. 7. It can be observed several bands in the regions from 590 to 1115 cm^{-1} refer to the vibrational mode PO_4^{3-} [23], indicating the formation of inorganic salts, as observed in the XRD analysis, the tricalcium phosphate phase. Bands in the regions between 1045-970 and 729 cm^{-1} indicate the asymmetric stretching of the P-O-P bond. Likewise, -a band in the region of 1250 cm^{-1}, typical of P=O, suggests the presence of the pyrophosphate group in coatings obtained according to DRX (Fig. 6). In all samples (0, 1 and 2) the presence of the band was verified at 3570 cm^{-1}, which is associated to stretching vibration of the OH group of the hydroxyapatite phase. In the fingerprint region, the presence of band assigments at 1630, 630 and 590 cm^{-1} were observed. These bands are associated to stretching of the OH group, the vibration of the PO_4^{3-} group and the unfolding of the PO_4^{3-} group, respectively, efering to the formation of the hydroxyapatite phase [25, 34]. In all samples submitted to the procedure (PB), two bands can be observed in the range of 1380–1460 cm^{-1}, which can be attributed to the vibrations of the CO_3^{2-} group, characterizing a possible result of atmospheric CO_2 chemisorption in the coating. The substitutions of type B with the carbonate ion, causes a distortion of the crystal network, contraction of the a-axis and expansion of the c-axis [25, 31].

Figure 8 shows the micrographies of samples 0, 1 and 2 after bioactive coatings, submitted to the procedure (PB). A mixture of agglomerate of spherical micro particles and dense plates was observed suggests the formation of phases HA and β-TCP, [23, 38].

4 Discussion

4.1 Laser surface irradiation

The complete laser-metal interaction cycle is complex and non-linear. The phenomena involved occur with simultaneous and sequential effects. There are three fundamental components in the interaction of the beam with the surface of the material: laminar melting, evaporation and breaking of chemical bonds. The infrared-laser emission with a wavelength of 1090 nm (Yb:YAG), allows both phenomena such as plasma production and ablation, which consists on submitting the metal surface to rapid fusion and solidification process [12, 28]. During the thermal cycle could be presented a sequence of chemical reactions of non-equilibrium conditions: beam absorption, laminar melting, instability in surface tensions, change in roughness pattern, plasma explosions, heat loss through conduction, oxidation and migration of impurities. Laser-modified samples showed the formation of rougher surfaces than those of titanium alloys, which is attributed to the higher energy density generated on the surface, producing a larger zone of fused metal.

In the Fig. 1, it can be observed the increased fluency, due to longer exposure time of the laser beam to the alloy

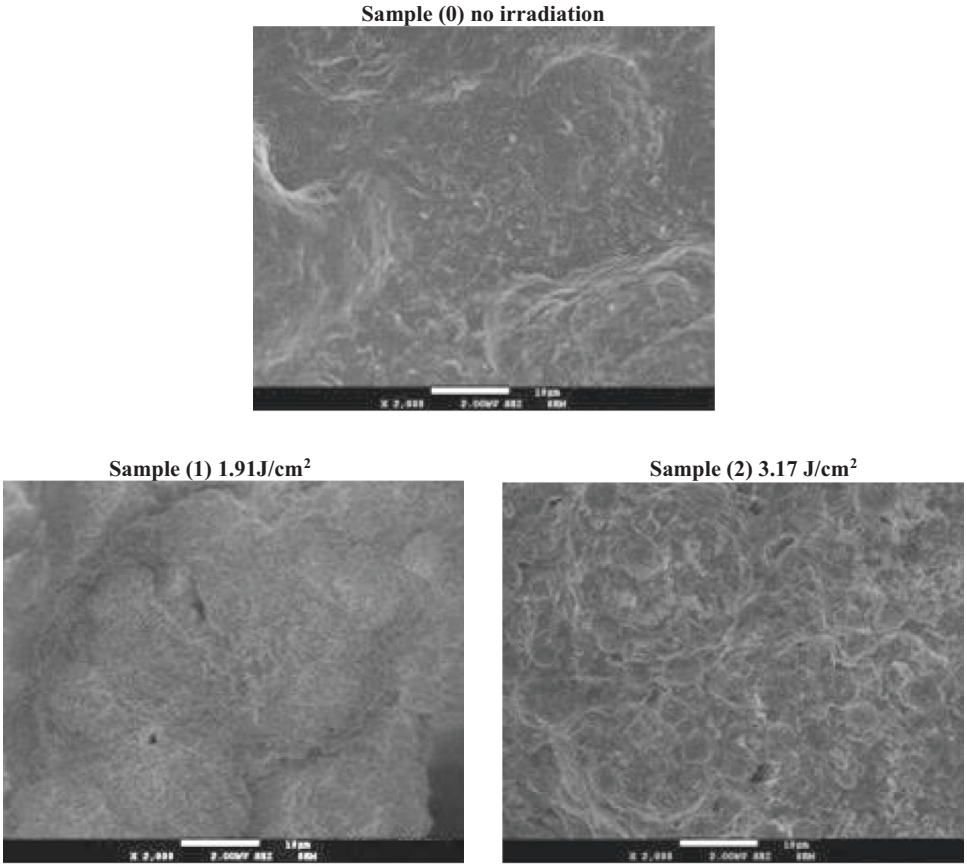

Fig. 5 SEM of the samples without irradiation (0) and (1) 1.91and (2) 3.17 J / cm^2 and after bioactive coating by the sol-gel method, procedure (PA), heat treatment at 350 °C. Magnitude 2000×

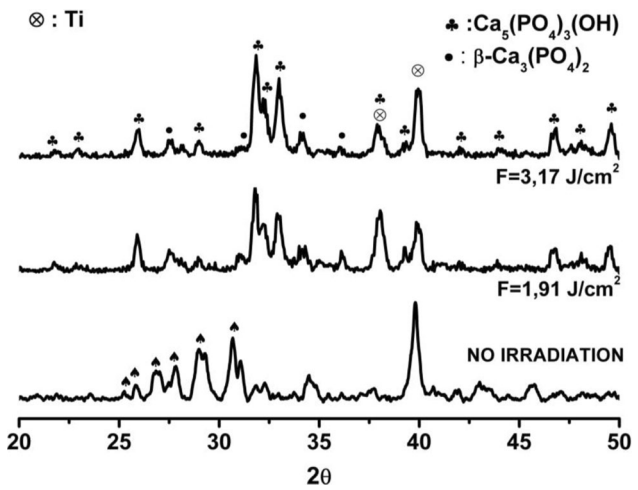

Fig. 6 X-ray diffraction of the samples after coating by the sol-gel method, procedure (PB), heat treatment at 600 °C. (0) no irradiation, samples (1) 1.91 and (2) 3.17 J/cm^2

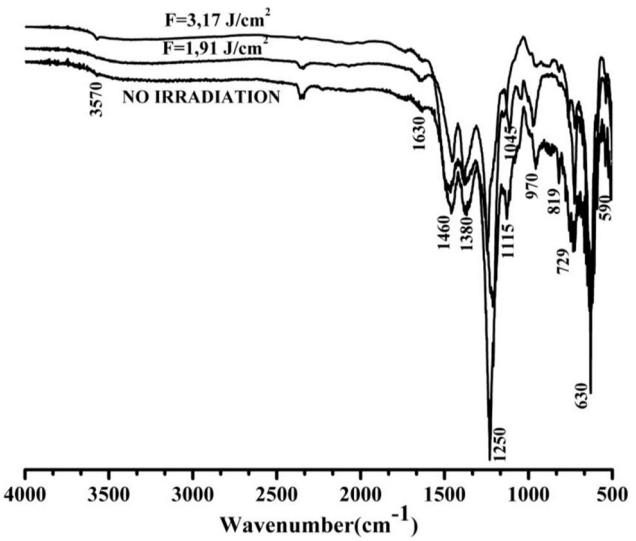

Fig. 7 Absorption spectrum in the medium infrared (FTIR) region of the samples after coating by the sol-gel method, procedure (PB), heat treatment at 600 °C. (0) no irradiation, samples (1) 1.91 and (2) 3.17 J/cm^2

surface, produces typical morphologies with different surface energies. This can be explain through the formation of new structures (metal oxides) produced during the fast melt and solidification process [16, 28].

Analyzing the Fig. 2 and Table 3, the results showed a rapid fusion and solidification process by laser beam irradiation under ambient air, inducing the formation of titanium oxides with different degrees of oxidation. It can be an indication that the laser energy favors the diffusion of O atoms (or N, depending on the atmospheric condition

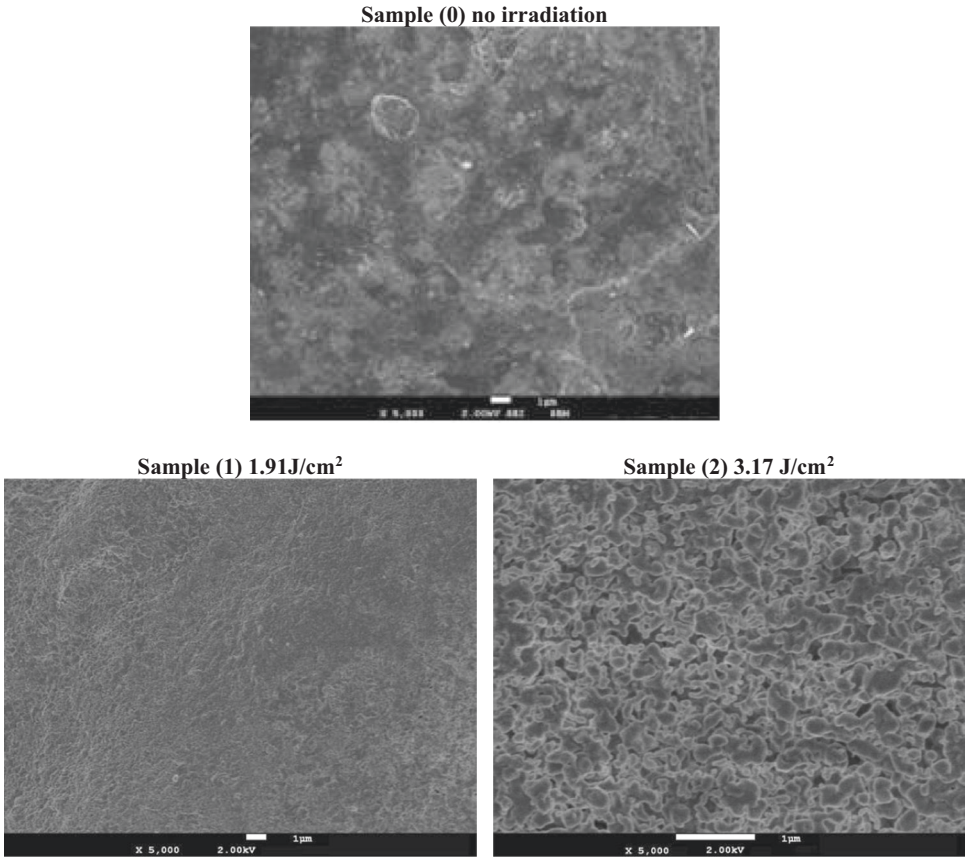

Fig. 8 SEM of the samples without irradiation (0) and (1) 1.91and (2) 3.17 J / cm^2 and after bioactive coating by the sol-gel method, procedure (PB), heat treatment at 600 °C

used), as well as the rapid solidification to form these phases in a condition of non-equilibrium. Ti_3O and Ti_6O oxides are classified as nonstoichiometric oxygen-deficient oxides, i.e., they have oxygen vacancies. These vacancies are defects; hence, they are deviations from the stoichiometric composition of compounds [39]. Nonstoichiometric phases are found in several oxide systems at high temperatures, particularly, for cations may have various states (valences) of oxidation [39]. The metallic titanium is heated between 400 and 600 °C under ambient pressure and air, in order to transforms into a TiO_{2-x} phases. The β-Ti phase occurs at high temperatures and low oxygen concentrations. Thus, the presence of the β-Ti cubic phase at the surface can be understood in terms of the low oxygen content in the central area of the laser beam incidence angle, due to the dispersion of molecules [40]. Another factor contributing to the formation of cubic phase is a rapid surface solidification process. The formation of β-TiO phase may be related to β-Ti phase [40]. The crystal lattice of titanium can absorb about 40% of atomic oxygen (18% w/w) in interstitial solid solution. The first intermediate phase, TiO, corresponds to all the forms of TiO_x (18-29.4 w/w). Before the region of formation of TiO_2 (40% w/w), a phase is formed with lower oxygen content, the titanium oxide series Ti_nO_{2n-1}, which encompasses the interval of (36% w/w) and comprises a large variety of species. The presence of the Ti_3O and Ti_6O substoichiometric phases can be explained by interstitial oxygen diffusion in the Ti lattice [39]. Due to the high solubility of oxygen in titanium, this property leads to the formation of a large quantity of oxides, with an O/Ti ratio within the interval of 0–2.

4.2 Coating using the sol gel method

4.2.1 Procedure (PA)—heat treatment at 350 °C

The procedure (PA) was used to obtain precursor phases, the formation of the monohydrogen calcium phosphate ($CaHPO_4$) and calcium pyrophosphate ($Ca_2P_2O_7$) phases are recognized as precursor phases of the hydroxyapatite phase, [31]. Thus, the heat treatment aims was elimination of organic compounds, derived from the nitrate anion present in the solution, leaving only the phases of interest in the substrate.

The Figs. 3,4 and 5 showed the samples irradiated with laser beam promote the formation of phases of calcium phosphates. Calcium pyrophosphate, Ca/P ratio = 1.0, belongs to the group of condensed phosphates, compounds

having P–O–P bond. These are formed by the condensation of monohydrogen calcium phosphate with increasing temperature, reactions 2 and 3 [20, 32].

$$2CaHPO_4.2H_2O \xrightarrow{393K} 2CaHPO_4 + 2H_2O \xrightarrow{723K} \gamma - Ca_2P_2O_7 + H_2O \quad (2)$$

$$\gamma - Ca_2P_2O_7 + H_2O \xrightarrow{1023K} \beta - Ca_2P_2O_7 \xrightarrow{1453K} \alpha - Ca_2P_2O_7 \quad (3)$$

According to the XRD, IR and SEM analyzes, it was indicated the formation of the phases, calcium pyrophosphate, HA and β-TCP.

4.2.2 Procedure (PB)—heat treatment at 600 °C

In order to obtain majority formation of the HA and β-TCP phases, the coatings were obtained by procedure (PB). Unlike the procedure (PA), the laser beam surface modification associated to thermal treatment at 600 °C allowed the formation of β-TCP (procedure PB). In the sol-gel process, the formation of the β-TCP phase may be related to the decomposition of the carbonated hydroxyapatite phase at high temperatures after heat treatment (reaction 4) [20, 25, 31, 41].

$$Ca_{10}(PO_4, CO_3)_6(OH)_2 \xrightarrow{\geq 600^\circ C} Ca_3(PO_4)_2 + Ca_{10}(PO_4)_6(OH)_2 + CO_2 \uparrow \quad (4)$$

According to Kanazawa [31] the process of formation of the β-TCP phase may be related to the decomposition of the non-stoichiometric hydroxyapatite phase, between 600 and 800 °C, reaction 5.

$$Ca_{10-x}(HPO_4)_x(PO_4)_{6-x}(OH)_{2-x}.nH_2O \rightarrow (1-x)Ca_{10}(PO_4)_6(OH)_2 + 3xCa_3(PO_4)_2 + H_2O_{(g)} \quad (5)$$

The result suggests the formation of phases HA and β-TCP, according to the XRD (Fig. 6), IR (Fig. 7) and SEM (Fig.8) analyzes. Therefore, the physico-chemical properties of the coatings on the Ti-15Mo surfaces, using the parameters of 1.91 and 3.17 J/cm^2 and procedure (PB), have indicated to be a promising strategy for orthopedic and dental implants. As well-know, besides hydroxyapatite, main component of the bone is collagen in the solid phase, the tricalcium phosphate phase (β-TCP) was obtained. This material is biodegradable, biocompatible and partially reabsorbed between 6 and 15 weeks after implant process, depending on the porosity and physicochemistry of the modified surface [42]. It can corroborate to application in hard tissue regeneration.

5 Conclusions

The laser beam-irradiated Ti-15Mo process has influenced the substrate/coating interactions, promoting a better interaction with the calcium and phosphate ions. In the two pre-established parameter conditions of the beam, the ablation process can occur. In this case, the rapid melting and the solidification step, under atmospheric conditions, have promote the formation of stoichiometric oxides TiO_2 and non-stoichiometric TiO, Ti_3O, Ti_3O_5 and Ti_6O with different oxide percentages, depending on the fluency applied. Laser beam modification is a clean and reproducible process, leaving no traces of contamination, as an important feature for clinical applications. By the results obtained from the bioactive coatings, it was possible to verify the influence of the heat treatment to obtain the calcium phospahtes phases. The results of the physico-chemical characterization showed for the procedure (PA) the formation of a mixture of phases—calcium pyrophosphate and β-TCP, whereas for the procedure (PB), it was obtained HA and β-TCP. The SEM analyzes showed different morphologies, both for the procedure (PB) and for the (PA), suggesting the different amounts of oxides formed by the laser beam influenced the morphology of the coatings. In general, it can be concluded the topographic profile and the physico-chemical properties of the surfaces were adequate for the reception of bioceramics coatings due to the formation of oxides diversity and irregular morphology; thus physicochemistry plays a fundamental role both in the ceramic coatings on the surface irradiated by laser and favors the phenomenon of osseointegration.

Acknowledgements The authors thank to the CNPQ and FAPESP by the financial support.

Compliance with ethical standards

Conflict of interest The authors declares that they have no conflict of interest.

References

1. Jan Henkel MA, Woodruff DR, Epari RS, Vaida G, Ian CD, Peter FM, Choong MA, Dietmar WH. Bone regeneration based on tissue engineering conceptions — A 21st century perspective. Bone Resv. 2013;3:216–48.
2. Park HH. Bioactive and electrochemical characterization of TiO_2 nanotubes on titanium via anodic oxidation". Electro Acta. 2010;55:6109–14.
3. Geetha M, Singh AK, Asokamani R, Gogia AK. Ti based biomaterials, the ultimate choice for orthopaedic implants – A review. Prog Mater Sci. 2009;54:397–425.
4. Ratner BD. Biomaterials: where we have been and where we are going. Annu Rev Biomed Eng. 2004;6:41–75.

5. Sasikumar Y. Influence of surface modification on the apatite formation and corrosion behavior of Ti and Ti-15Mo alloy for biomedical applications. Mat Chem Phy. 2013;138:114–23.
6. Sasikumar Y. In vitro bioactivity of surface- modified β-Ti alloy for biomedical applications. J Mat Eng Perf. 2011;20:1271–7.
7. Oliveira NTC. Electrochemical stability and corrosion resistance of Ti-Mo alloys for biomedical applications. Acta Biomat. 2009;5:399–405.
8. Oliveira NTC. Photo-electrochemical investigation of anodic oxide films on as-cast Ti-Mo alloys. I. Anodic behaviour and effect of alloy composition. Electro Acta. 2009;54:1395–402.
9. Oliveira NTC. Laser-treated Ti-15Mo alloy for biomedical applications: in vivo studies in a rabbit model using biomechanical, hystological and histomorphometrical analysis. Clin Implant Dentristy Relat Res. 2011;15:427–37.
10. Oliveira NTC. In vitro analysis with human bone marrow stem cells on Ti-15Mo alloy for dental and orthopedic implants application. J Osseoint. 2011;3:27–33.
11. Yoshiki O, Elif BT, Oya A, Koray G. Dental Implant Systems. Int J Mol Sci. 2010;11:1580–678.
12. Silfvast WT. Laser fundamentals. Cambridge: Cambridge University Press; 1996.
13. Zhennan D, Baodi Y, Weihong L, Jinsong L, Jingyuan Y, Tieli Z, Dafeng Z, Haiyang Y, Xiaoguang L, Jianfeng M. Surface characteristics of and in vitro behavior of osteoblast-like cells on titanium with nanotopography prepared by high-energy shot peening. Int J Nanom. 2014;9:5565–73.
14. Anselme K. Osteoblast adhesion on biomaterials. Biomaterials. 2000;21:667–81.
15. Queiroz TP. Commercially pure titanium implants with surfaces modified by laser beam with and without chemical deposition of apatite. Biomechanical and topographical analysis in rabbits. Clin Oral Implants Res. 2013;24:896–903.
16. Lavisse L. The early stage of the laser-induced oxidation of titanium substrates. Appl Surf Sci. 2002;186:150–5.
17. Pérez del PA. Oxidation of titanium through Nd:YAG laser irradiation. Appl Surf Sci. 2002;197-198:887–90.
18. Gareth JO, Rajendra KS, Farzad F, Mustafa A, Cheol-Min H, Chinmaya M, Hae-Won K, Jonathan CK. Sol–gel based materials for biomedical applications. Prog Mater Sci. 2016;77:1–79.
19. Živilė S, Milda M, Aldona B, Aivaras K. Sol-gel synthesis of calcium phosphate coatings on Ti substrate using dip-coating technique. Chemija. 2013;24:288–95.
20. Windarti T, Taslimah AH, Astuti1 Y, Darmawan A (Synthesis of β-Calcium Pyrophosphate by sol-gel method. IOP Conf. Series: Mater Sci Eng. 2017. https://doi.org/10.1088/1757-899X/172/1/012058.
21. Eshtiagh HH. Preparation of anhydrous dicalcium phosphate, DCPA, through sol–gel process, identification and phase transformation evaluation. J Non-Cryst Solids. 2008;354:3854–7.
22. Bezzi A. A novel sol-gel technique for hydroxyapatite preparation. Mat Chem Phys. 2003;78:816–24.
23. Liu DM. Sol-gel hydroxyapatite coatings on stainless steel substrates. Biomaterials. 2002;23:691–8.
24. Mavis B, Tas C. Dip coating of calcium hydroxyapatite on Ti-6Al-4V substrates. J Am Ceram Soc. 2000;83:989–91.
25. Hwang K, Lim Y. Chemical and structural changes of hydroxyapatite films by using a sol-gel method. Surf Coat Technol. 1999;115:172–5.
26. Ellingsen JE. Bio-implant interface. New York: CRC; 2003.
27. Kasemo B. Biocompatibility of titanium implants: surface science aspects. J Prost Dent. 1983;49:832–7.
28. Braga FJC. Surface modification of Ti dental implants by Nd: YVO4 laser irradiation. Appl Surf Sci. 2007;253:9203–8.
29. Joint Committee on Powder Diffraction Standards (JCPDS)/ International Center for Diffraction Data-ICDD, Hanawalt Search Manual / Inorganic Phases, Powder Diffraction File, Sets 1-52, JCPDS/ICDD, Pennsylvania, 2003.
30. Rietveld HM. A profile refinement method for nuclear and magnetic structures. J Appl Cryst. 1969;2:65–71.
31. Kanazawa T. Inorganic phosphate materials.. Tokio: Elsevier; 1989.
32. Durif A. Crystal chemistry of condensed phosphate. New York: Plenum Press; 1995.
33. Li Microstructure K. in vitro corrosion and cytotoxicity of Ca-P coatings on ZK60 magnesium alloy prepared by simple chemical conversion and heat treatment. J Biomat Appl. 2013;28:375–84.
34. Chen J. A simple sol-gel technique for synthesis of nanostructured hydroxyapatite, tricalcium phosphate and biphasic powders. Mat Let. 2011;65:1923–6.
35. Breding K. The effect of hydroxyapatite nanocrystals on osseointegration of titanium implants: An in vivo rabbit study. Int J of Dent. 2014; https://doi.org/10.1155/2014/171305.
36. Driessens FCM. Biological calcium phosphates and their role in the physiological of bone and dental tissue. Composition and solubility of calcium phosphates. Calcif Tissue Res. 1978;26:127–37.
37. You C. Influences of heating condition and substrate-surface roughness on the characteristics of sol-gel derived hydroxyapatite coatings. J Sol-Gel Sci Techn. 2001;21:49–54.
38. Hsieh MF. Hydroxyapatite coating on Ti6Al4V alloy using a sol-gel derived precursor. Mat Chem Phys. 2002;74:245–50.
39. Sorensen OT. Nonstoichiometric oxides. New York: Academic Press; 1981.
40. György E. Chemical composition of dome-shaped structures grown on titanium by multi-pulse Nd:YAG laser irradiation. Appl Surf Sci. 2004;222:415–22.
41. RZ Legeros, JP Legeros In: Hench LL, Wilson J (eds) Dense hydroxyapatite. An Introduction to Bioceramics. 1:139-180. ISBN 981-02- 1400-6, Singapore, October 1993. https://doi.org/10.1142/9789814317351_0009.
42. Oréfice RL. Biomateriais: fundamentos e aplicações. Rio de Janeiro: Cultura Médica; 2006.